Supporting Information

Maximizing Magnetic Resonance Contrast in Gd(III) Nanoconjugates: Investigation of Proton Relaxation in Zirconium Metal–Organic Frameworks

Shaunna M. McLeod,[†,#] Lee Robison,[‡,#] Giacomo Parigi,[§] Alyssa Olszewski,[‡] Riki J. Drout,[‡] Xinyi Gong,[‡] Timur Islamoglu,[‡] Claudio Luchinat,[§] Omar K. Farha,[*,‡] Thomas J. Meade*[,†]

Affiliations:

[†]Departments of Chemistry, Molecular Biosciences, Neurobiology, and Radiology, Northwestern University, Evanston, Illinois 60208, United States

[‡]International Institute of Nanotechnology, Department of Chemistry, Northwestern University, Evanston, Illinois 60208, United States

[§]Magnetic Resonance Center (CERM), Consorzio Interuniversitario Risonanze Magnetiche di Metalloproteine (CIRMMP) and Department of Chemistry, University of Florence, 50019 Sesto Fiorentino, Italy

[#] S.M.M. and L.R. contributed equally.

*Correspondence to: tmeade@northwestern.edu; o-farha@northwestern.edu

Contents

Experimental Methods & Instrumentation

Ambient pressure powder X-ray Diffraction (PXRD) data were collected at the IMSERC X-ray Facility at Northwestern University on a STOE-STADI-MP powder diffractometer equipped with an asymmetric curved Germanium monochromator (CuKα1 radiation, λ = 1.54056 Å) and one-dimensional silicon strip detector (MYTHEN2 1K from DECTRIS). The line focused Cu X-ray tube was operated at 40 kV and 40 mA. Powder was packed in a 3 mm metallic mask and sandwiched between two layers of polyimide tape. Intensity data from 2 to 30 degrees 2θ were collected over a period of 10 mins. The instrument was calibrated against a NIST Silicon standard (640d) prior the measurement.

N_2 adsorption and desorption isotherms were measured on a Micromeritics Tristar II 3020 (Micromeritics, Norcross, GA) instrument at 77 K. Pore-size distributions were obtained using DFT calculations using a carbon slit-pore model with a N_2 kernel in Micromeritics MicroActive software. Before each run, samples were activated at 120 °C for 16–24 hr under high vacuum on a Smart Vacprep from Micromeritics. Approximately 40 mg of sample was used in each measurement and Brunauer–Emmett–Teller (BET) surface area was calculated in the region P/P_0 = 0.005–0.05.

Scanning electron microscopy (SEM) images were collected on a Hitachi SU8030 FE-SEM microscope with a field emission gun (Dallas, TX) at Northwestern University's EPIC/NUANCE facility. Before imaging, samples were coated with OsO_4 to ~9 nm thickness in a Denton Desk III TSC Sputter Coater (Moorestown, NJ).

Scanning transmission electron microscopy energy-dispersive X-ray spectroscopy (STEM-EDS) images and analyses were performed using a JEOL ARM200CF operated at 200 keV and acquired with probe size 8C and camera length 20 cm.

Diffuse reflectance infrared spectra (DRIFTS) were recorded on a Nicolet 6700 FTIR spectrometer equipped with a MCT detector. DRIFTS spectra of MOFs were collected using a sealed chamber with IR transparent ZnSe windows. The detector was cooled with liquid N2. A spectral resolution of 1 cm—1 was used and the reported spectra are average of 64 scans. Samples were heated at 120

°C under Ar flow prior to spectra collection to remove physisorbed water and other solvent residuals, and then cooled down to 30 °C for data collection. KBr was utilized as a background spectrum.

For Gd(III) complex purification and characterization, thin-layer chromatography (TLC) was performed on EMD 60 F254 silica gel plates. Standard grade 60 Å 230–400 mesh silica gel was used for normal-phase column chromatography. ^{1}H and ^{13}C NMR spectra were obtained on a Bruker 500 MHz Avance III NMR spectrometer. ESI-MS was performed on a Bruker AmaZon-SL spectrometer. Analytical HPLC-MS was performed on an Agilent 1260 Infinity II HPLC system with an in-line Agilent 6120 Quad mass spectrometer. Semi-preparative HPLC was performed on an Agilent PrepStar 218 equipped with an Agilent 1260 Infinity diode array detector. HPLC purifications utilized deionized water (18.2 MΩ·cm) obtained from a Millipore Q-Guard System and HPLC grade acetonitrile (obtained from Fisher Scientific). Analytical HPLC-MS used an Atlantis C18 column (4.6 × 250 mm, 5 μm). Semipreparative HPLC used an Atlantis T3 C18 column (19 x 250 mm, 10 μm).

Zr-MOF Syntheses

All MOF samples were thermally activated under ultrahigh vacuum at 120 °C for 12 h on a Micromeritics Smart VacPrep. MOF NMR samples were prepared by digesting ~1-2 mg with 5 drops of D_2SO_4 and diluting with 2 mL DMSO-d^6 for ^{1}H-NMR spectra.

Synthesis of NU-1000

NU-1000 was prepared according to a literature procedure.[1] Specifically, $ZrOCl_2.8H_2O$ (9.7 g, 30 mmol) and benzoic acid (200 g, 1.6 mol) were mixed in 600 mL of DMF in a 2-L glass bottle and ultrasonically dissolved. The clear solution was incubated in an oven at 100 ^{0}C for 1 hr. H_4TBAPy (4 g, 6 mmol) was added to 200 mL DMF and heated to 100 ^{0}C for 1 hr. After cooling down to room temperature, H_4TBAPy solution and trifluoroacetic acid (TFA) (4 mL, 52 mmol) were added to the pre-made Zr-node solution and sonicated for 10 min. The suspension was placed into an oven at 120 ^{0}C for 18 hr. After cooling down to room temperature, yellow polycrystalline material was collected into six 50-mL centrifuge tubes by multiple cycle of centrifugation (5 min, 7500 rpm) and washed with dimethlyformamide (DMF) three times (~300 mL each) (soaked ~1 hr between washes). An HCl washing step was performed to remove modulator from the node. The resulting yellow powder was suspended in 1300 mL DMF in a 2-L glass bottle and 50 mL of 8 M aqueous HCl was added. This mixture was heated in an oven at 100 ^{0}C for 18 hr. After cooling to room temperature, the powder was isolated by centrifugation and washed with dimethlyformamide (DMF) three times (~300 mL each) and acetone three times (~300 mL each) (soaked ~1 hr between washes) and soaked in acetone for an additional 16 hr. NU-1000 crystals were collected by centrifugation and dried in a vacuum oven at 80 ^{0}C for 1 hr before activation on a Micromeritics Smart VacPrep instrument. (yield: ~5.5 g activated NU-1000). (200 mg and 2 g scale synthesis can be performed following this procedure by scaling down all reagents accordingly.)

Synthesis of nano NU-1000

Nano NU-1000 was prepared according to a previously reported procedure.[2] $ZrOCl_2.8H_2O$ (970 mg, 3.0 mmol) and benzoic acid (16.0 g, 131 mmol) were mixed in 80 mL of DMF and incubated in an oven at 100 ^{0}C for 1 hr. H_4TBAPy (200 mg, 0.300 mmol) was added to 80 mL of DMF and heated to 100 ^{0}C for 1 hr. After cooling down to room temperature, 1 mL of the zirconium solution and 1 mL of the node solution were added to a 1.5-dram vial containing 20 μL trifluoroacetic acid (0.26 mmol), resulting in a translucent yellow solution. Ten sample vials were prepared under the same conditions and placed into an oven at 100 °C for 1 hr, during which time a yellow suspension formed. After cooling to room temperature, the 10 vials were combined, and the suspension was isolated by centrifugation at 7800 rpm for 10 min. The sample was further washed with DMF and acetone twice, then subsequently activated with HCl. Approximately 50 mg of sample was soaked in 20 mL of DMF and 4 mL of 8 M aqueous HCl was added. This mixture was heated in an oven at 100 °C for 24 h. After cooling to room temperature, the filtrate was decanted, and the material was washed twice with DMF to remove HCl impurities. Subsequently, the solid residue was washed with acetone (2×) and soaked in acetone for an additional 12 hr. The solid was filtered, briefly dried on a filter paper and activated at 120 °C under vacuum for 12 hr before adsorption measurements.

Synthesis of NU-901

NU-901 was prepared according to literature procedure with slight modifications.[3] These changes included a scale up to 5x of the previously reported synthesis and fully solubilizing the 4-

aminobenzoic acid modulator in the *N,N*-dimethylformamide (DMF) before the addition of the $Zr(acac)_4$, which was achieved by sonication and heating at 100°C for increments of 10 minutes until the modulator fully dissolved. The ligand for NU-901, 1,3,6,8-tetrakis(p-benzoic acid)pyrene (H_4TBAPy), was synthesized by a published procedure. All MOF samples were thermally activated under ultrahigh vacuum at 120 °C for 18 hr on a Micromeritics Smart VacPrep. Nitrogen adsorption and desorption isotherm measurements were performed on a Micromeritics Tristar II at 77 K to verify their porosity. Ambient pressure powder X-ray diffraction measurements were collected on a STOE STADI MP equipped with Kα1 source and a 1D strip detector over a range of $2° < 2\theta < 37°$ to confirm their crystallinity.

Zirconium and Gadolinium Analysis by ICP-OES

To calculate the Gd-C5-COOH complex loading in each MOF, quantification of Gd and Zr was accomplished using inductively coupled plasma-optical emission spectrometry (ICP-OES) of acid digested samples. Specifically, solid samples (1-2 mg) of the Gd(III)-functionalized Zr-MOFs were digested using a Milestone Ethos EZ Microwave Digestion System. Samples were digested in a mixture of 2 mL concentrated trace nitric acid (> 69%, Thermo Fisher Scientific, Waltham, MA, USA) and 0.5 mL trace hydrogen peroxide (> 30%, GFS Chemicals, Columbus, OH, USA) and were microwaved for 30 minutes at 200 °C, with a 15 minute ramp time and a 30 minute exhaust time. Ultra-pure H_2O (18.2 MΩ·cm) was added to produce a final solution of 3.0% nitric acid (v/v). Quantitative standards consisting of 10, 5, 2.5, 1.25, 0.625, and 0.3125 µg/g were made using a 10,000 µg/mL Gd elemental standard and a 1,000 µg/mL Zr elemental standard (Inorganic Ventures, Christiansburg, VA, USA) in 3.0% nitric acid (v/v) in a total sample volume of 5 mL. ICP-OES was performed on a computer-controlled (QTEGRA software) Thermo iCap7600 ICP-OES (Thermo Fisher Scientific, Waltham, MA, USA) operating in radial view and equipped with a CETAC 520 autosampler (Omaha, NE, USA). Each sample was acquired using 5 second visible exposure time and 15 second UV exposure time, running 3 replicates. The spectral lines selected for analysis were: Zr (343.823, 327.305, 349.621 nm), and Gd (335.047, 336.223, 342.247, 310.050 nm). Loading was calculated using the ratio of $Gd:Zr_6$, or complexes per node in the MOF material.

Relaxivity at 1.4 T

A stock suspension of each Gd(III)-functionalized Zr-MOF sample was made by suspending approx. 1 mg of material in 1 mL of Millipore water. Suspension was achieved through bath sonication and vortexing for periods of 10 min each. This sample was serially diluted four times, generating five samples of 500 µL each, and heated to 37 °C. Relaxation times were measured on a Bruker mq60 NMR analyzer equipped with Minispec v 2.51 Rev.00/NT software (Bruker Biospin, Billerica, MA, USA) operating at 1.41 T (60 MHz) and 37 °C. Measurement of T_1 relaxation times were made using an inversion recovery pulse sequence using the following parameters: 4 scans per point, 10 data points, mono-exponential curve fitting, phase cycling, 10 ms first pulse separation, and a recycle delay and final pulse separation $\geq 5\ T_1$. Measurement of T_2 relaxation times were made using the Carr-Purcell-Meiboom-Gill (CPMG) pulse sequence. The inverse of the relaxation time ($1/T_1$ or $1/T_2$, s^{-1}) was plotted against the Gd(III) concentration (mM) determined by ICP-MS for each of the five samples. By applying a linear fit to this data, the slope generated was defined as the relaxivity (r_1, r_2) of the agent in units of $mM^{-1}\ s^{-1}$.

Relaxivity at 7 T

A stock suspension of each Gd(III)-functionalized Zr-MOF sample was made by suspending approx. 0.5 mg of material in 200 µL of Millipore water. Each sample was serially diluted to make a total of three solutions of varying concentration. A 50 µL aliquot of each solution was then pipetted into flame sealed Pasteur pipettes. The pipette tips containing solution were scored, separated, and sealed with parafilm to make small capillaries containing solution. These capillaries were imaged using a Bruker PharmaScan 7 T MR imaging spectrometer (Bruker BioSpin, Billerica, MA, USA). T_1 relaxation times were measured using a rapid-acquisition rapid-echo (RARE-VTR) T_1-map pulse sequence with static TE (10 ms) and variable TR (100, 200, 400, 500, 750, 1000, 2500, 7500, and 1000 ms) values. Imaging parameters were as follows: field of view, 25 x 25 mm^2; matrix size, 256 x 256; number of axial slices, 5; slice thickness, 1.0 mm; and averages, 4. T_2 relaxation times were measured using a multislice multiecho (MSME) T_2-map pulse sequence, with static TR (5000 ms) and 32 fitted echoes in 11 ms intervals (11, 22,..., 352 ms). Imaging parameters were as follows: field of view, 25×25 mm^2; matrix size, 256×256; number of axial slices, 4; slice thickness, 1.0 mm; and averages, 3. T_1 and T_2 analysis was carried out using the image sequence analysis tool in Paravision 6.0 software (Bruker) with mono-exponential curve-fitting of image intensities of selected ROIs for each axial slice.

Analysis of Gadolinium by ICP-MS

Quantification of Gd in relaxivity samples was accomplished using inductively coupled plasma mass spectrometry (ICP-MS) of acid digested samples. Specifically, 10 µL of each MOF suspension was digested in 300 µL concentrated trace nitric acid (> 69%, Thermo Fisher Scientific, Waltham, MA, USA) and placed at 65 °C for at least 3 hours to allow for complete sample digestion. Ultrapure H_2O (18.2 MΩ·cm) was then added to produce a final solution of 3.0% nitric acid in a total sample volume of 10 mL. Quantitative standards were made using a 10,000 µg/mL Gd elemental standard (Inorganic Ventures, Christiansburg, VA, USA) which were used to create a 200 ng/g element standard in 3.0% nitric acid (v/v) in a total sample volume of 50 mL. A solution of 3.0% nitric acid (v/v) was used as the calibration blank. ICP-MS was performed on a computer-controlled (QTEGRA software) Thermo iCapQ ICP-MS (Thermo Fisher Scientific, Waltham, MA, USA) operating in STD mode and equipped with an ESI SC-2DX PrepFAST autosampler (Omaha, NE, USA). Internal standard was added inline using the prepFAST system and consisted of 1 ng/mL of a mixed element solution containing Bi, In, ^{6}Li, Sc, Tb, Y (IV-ICPMS-71D from Inorganic Ventures). Online dilution was also carried out by the prepFAST system and used to generate a calibration curve consisting of 200, 100, 50, 10, 2, 1 ppb Gd and Zr. Each sample was acquired using 1 survey run (10 sweeps) and 3 main (peak jumping) runs (40 sweeps). The isotopes selected for analysis were ^{156,157}Gd, and ^{115}In, ^{159}Tb (chosen as internal standards for data interpolation and machine stability). Instrument performance is optimized daily through autotuning followed by verification via a performance report (passing manufacturer specifications).

Previously Reported Gd(III)-based MOF Contrast Agents

Table S1. Selected Gd(III)-based MOF MRI Contrast Agents

Reference No.	Gd(III) Incorporation Method	Other Relevant Functionalization	Relaxivity ($mM^{-1}s^{-1}$)	Field Strength (T)	Medium
4	Gd^{3+} ions as MOF nodes	*Polymer Coating:* No coating PHPMA (5327 g/mol) PHMPA (10281 g/mol) PHMPA (19370 g/mol) PNIPAM (5690 g/mol) PNIPAM (8606 g/mol) PNIPAM (17846 g/mol) PSty (4802 g/mol) PSty (8972 g/mol) PSty (15245 g/mol) PDMAEA (15120 g/mol) PPEGMEA (19542 g/mol) PAA (10888 g/mol) *Particle Size:* 122 ± 30 nm Platelets	 9.86 17.81 32.94 105.36 20.27 46.99 62.51 1.17 1.20 3.91 37.20 59.93 21.30	1.5	Deionized Water
5	Gd^{3+} ions as MOF nodes	*Particle Size:* 24 nm Rods 82 nm 112 nm 146 nm 207 nm 527 nm 1001 nm	 70.1 83.9 69.3 31.4 29.4 22.1 17.8	4.7	0.2% xanthan gum solution in water
6	Gd^{3+} ions as MOF nodes	200 nm Rods	15	0.6	pH 7.4 saline solution

Ref. 7 provides an overview of reported Gd(III)-based MOF MRI contrast agents. Apart from the MOFs described in ref. 4 and 5, reported relaxivity values for Gd(III)-based MOF CAs range from 5-35 $mM^{-1}s^{-1}$ (across a several of field strengths, see Table 2 in Ref. 7).

Ref. 4 and 5 demonstrate particularly exceptional MR relaxation enhancement. Ref. 4 shows enhanced relaxivities for Gd(III)-MOFs due to hydrophilic polymer coatings, with hydrophobic coating PSty for comparison. Relaxation enhancement also scales with polymer molecular weight in thus study (likely a τ_R effect). Ref. 5 showed a positive correlation between the surface areas of Gd(III)-MOF particles and relaxivity. However, neither study pursued more advanced relaxometry techniques to further characterize relaxation mechanisms. Ref. 6 is a rare MOF MRI CA study that uses NMRD techniques to investigate the relaxivity of the material across a range of field strengths and temperatures. The maximum relaxivity achieved for this material is 15 $mM^{-1}s^{-1}$ at 40 MHz and 25°C (0.6 T).

Powder X-ray Diffraction Data

(A)

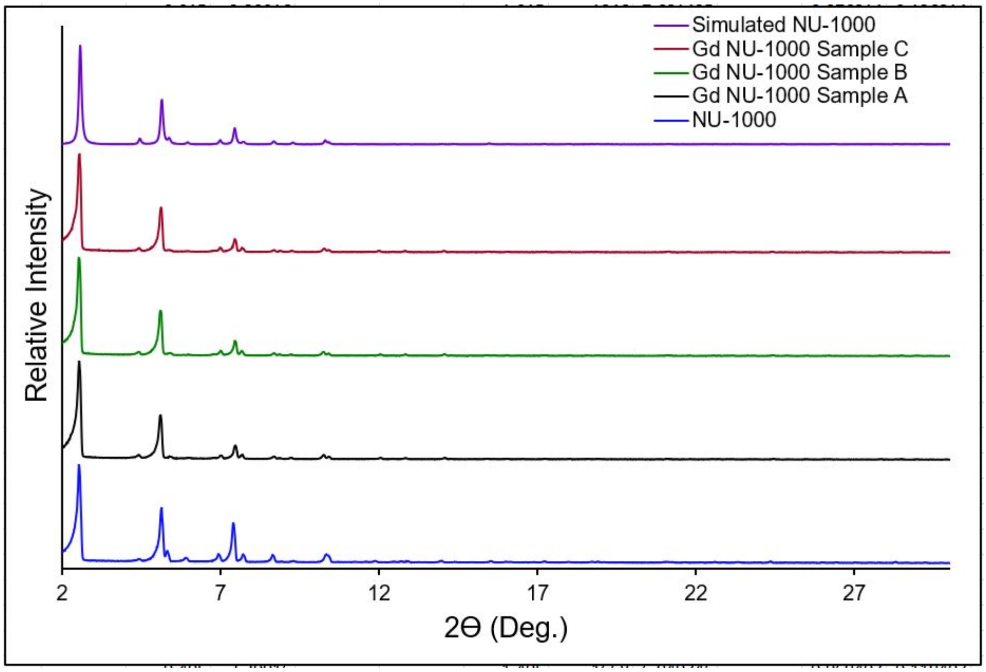

(B)

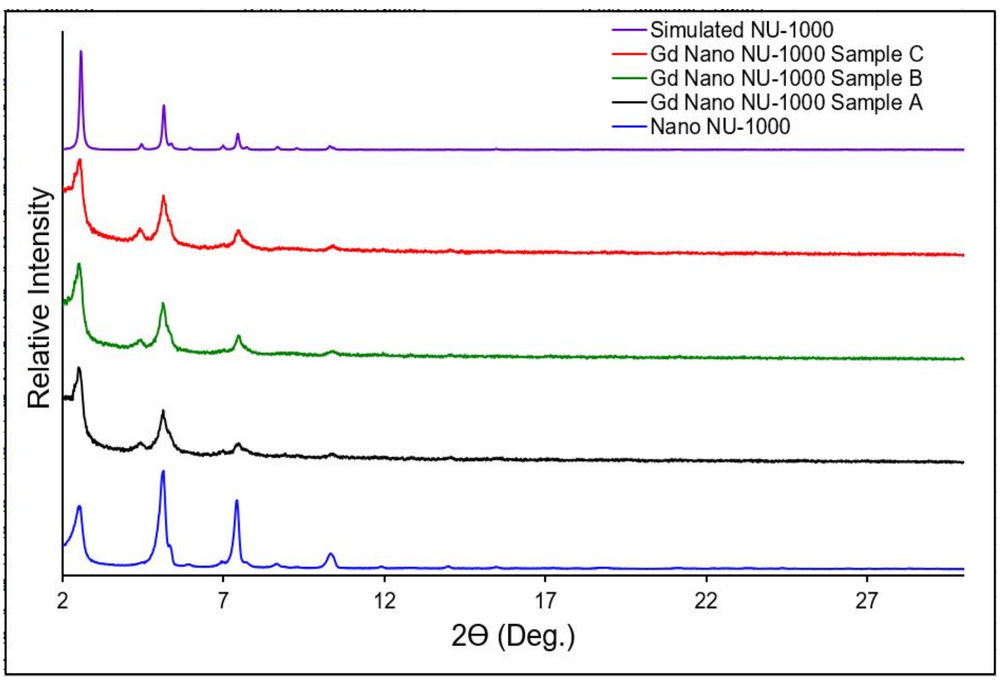

(C)

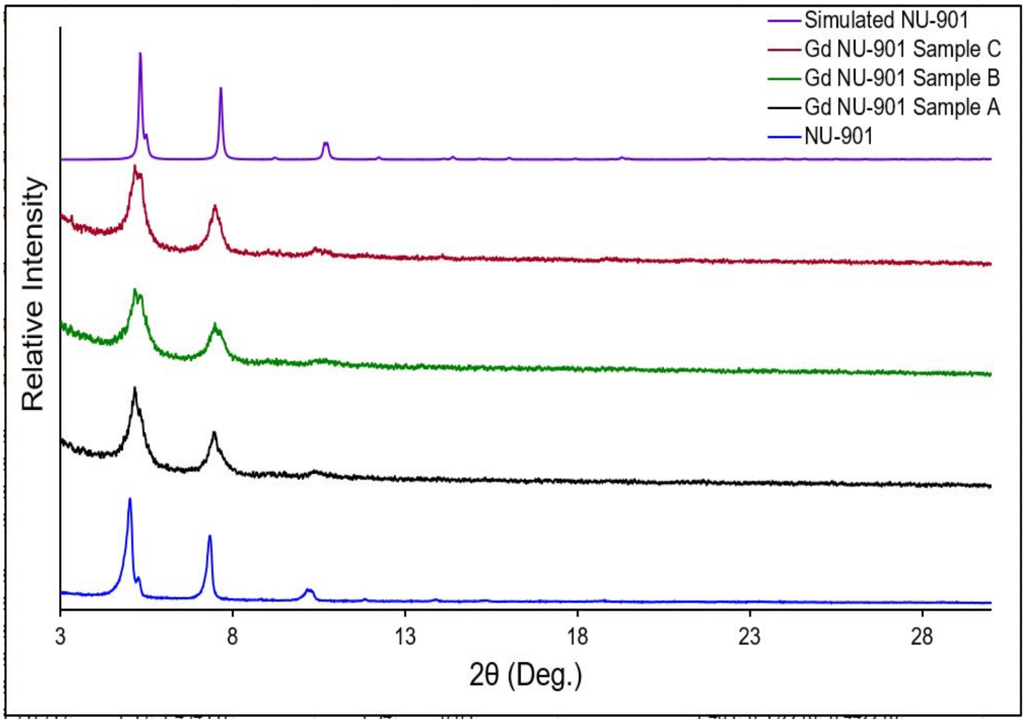

Figure S1. PXRD patterns of MOF series post-SALI. (A) NU-1000, (B) nano NU-1000, and (C) NU-901. Patterns show that crystallinity is maintained after functionalization with the Gd-C5-COOH complex.

Scanning Electron Microscopy Images

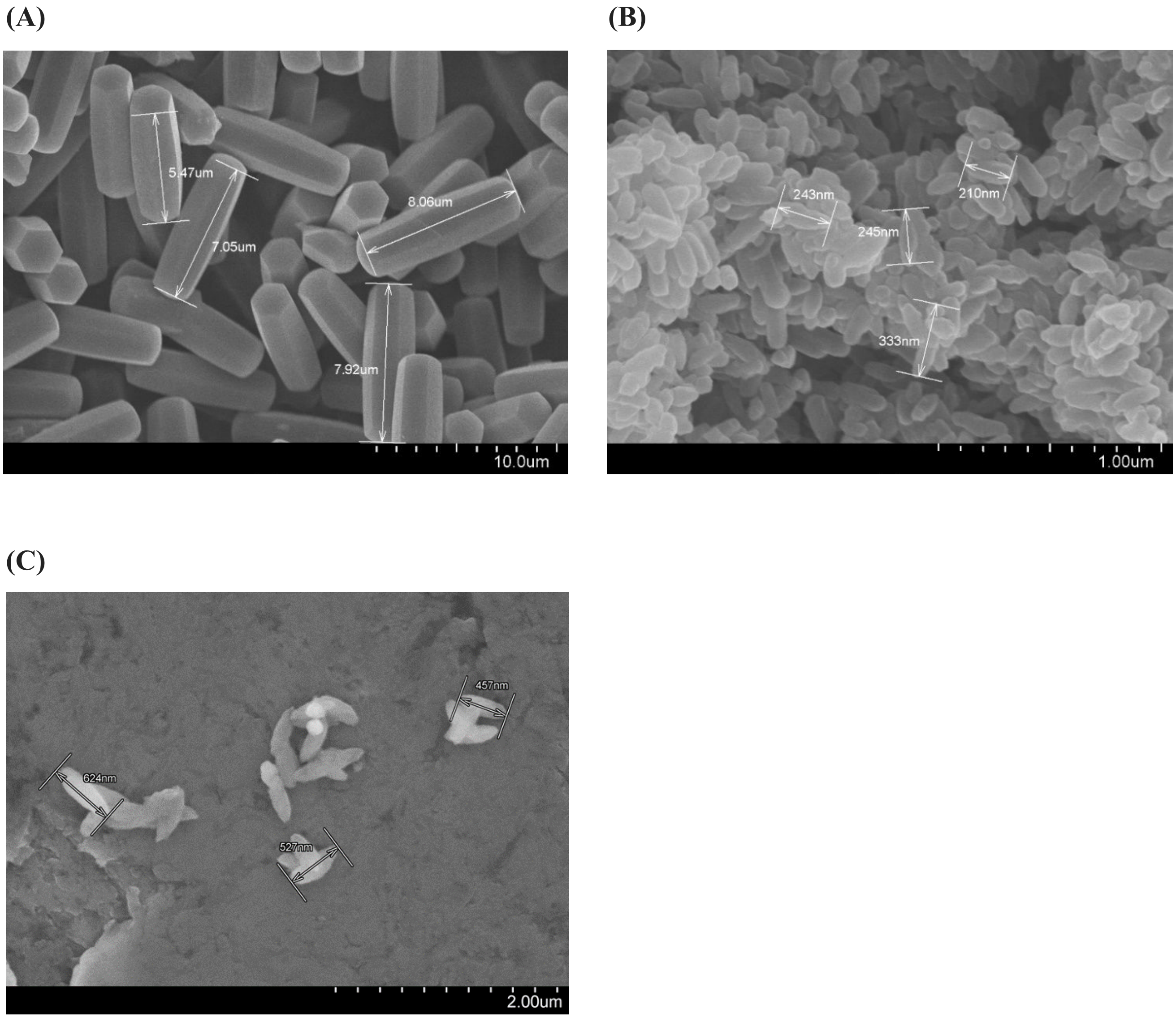

Figure S2. SEM images of unfunctionalized MOFs (A) NU-1000, (B) nano NU-1000, and (C) NU-901 particles. NU-1000 exhibits rods ~5.5-8 μm in length, nano NU-1000 exhibits much smaller 200-350 nm length particles and NU-901 particles are between 450-650 nm in length.

(A)

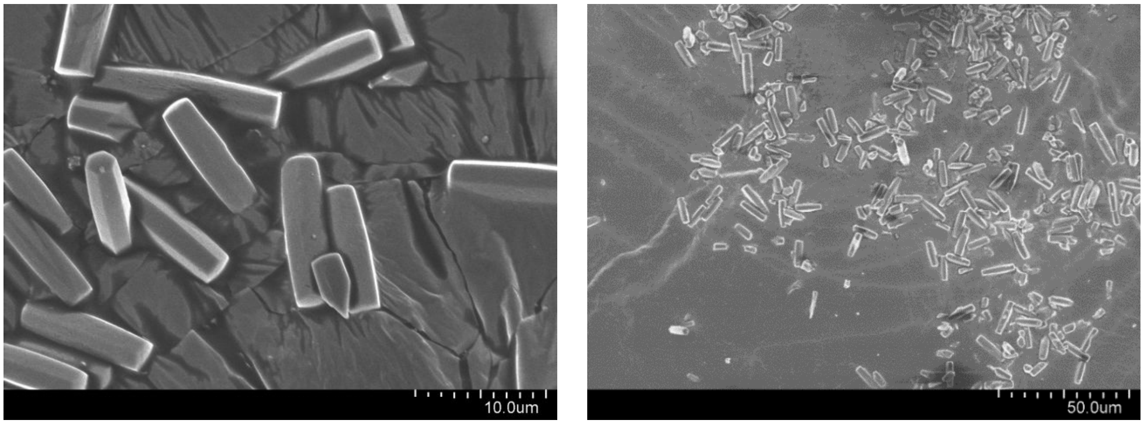

(B)

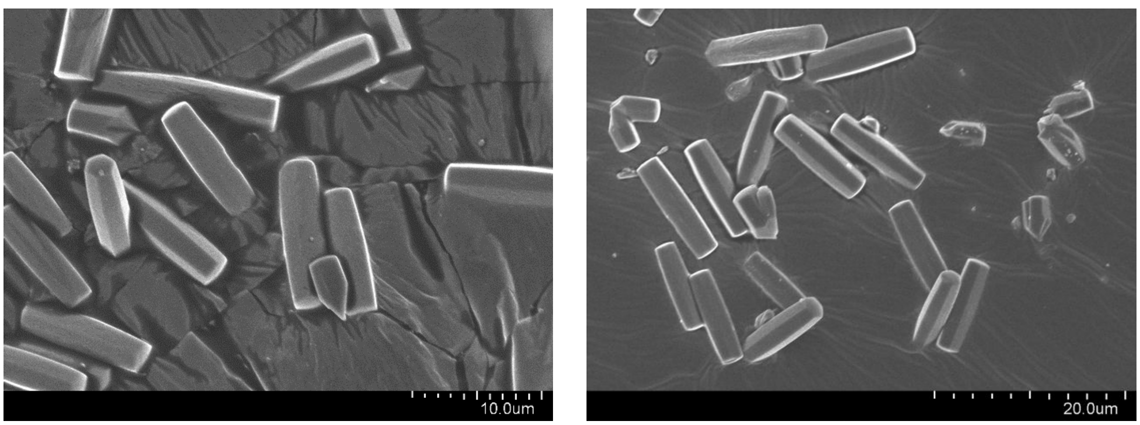

(C)

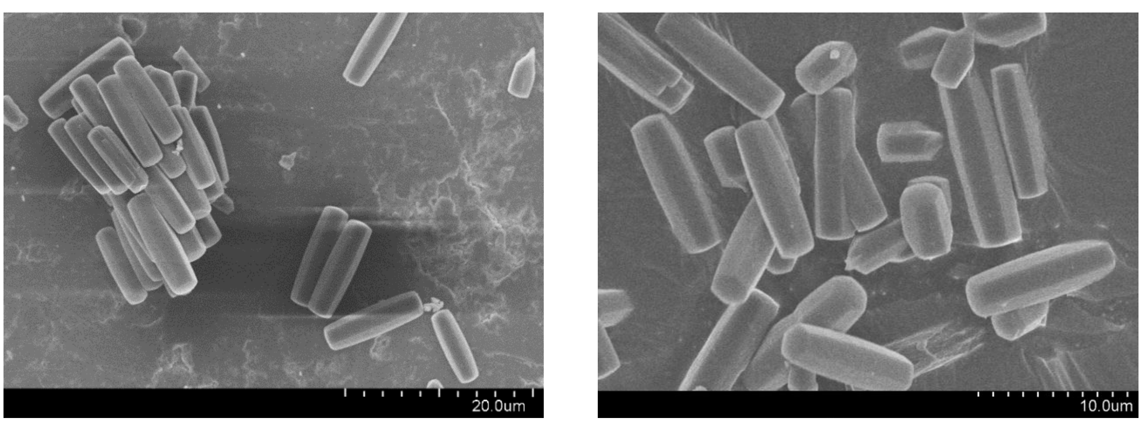

Figure S3. SEM images of Gd NU-1000. Sample A (top 2), Sample B (middle 2) and Sample C (bottom two). No change is observed in particle morphology after SALI.

(A)

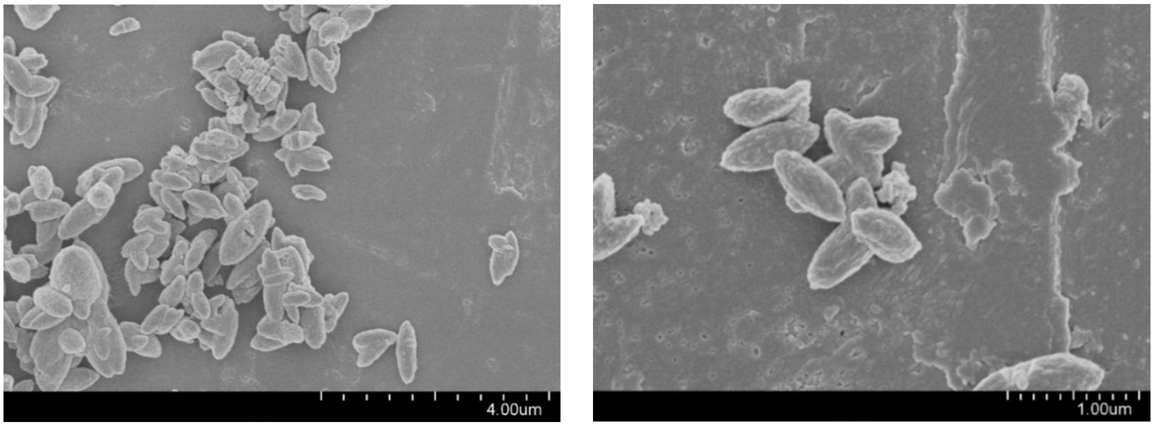

(B)

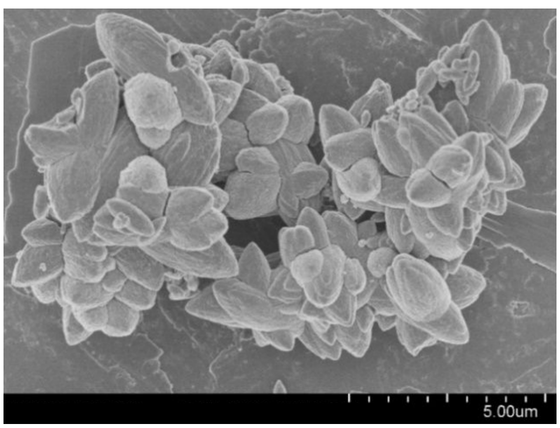

(C)

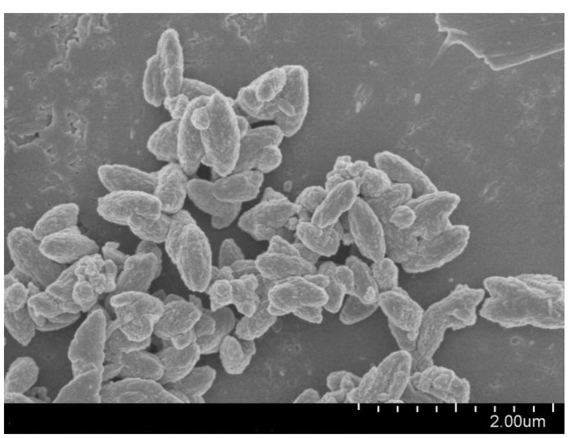

Figure S4. SEM images of three batches of Gd NU-901. Sample A (top 2), Sample B (middle left) and Sample C (bottom left). No change is observed in particle morphology after SALI.

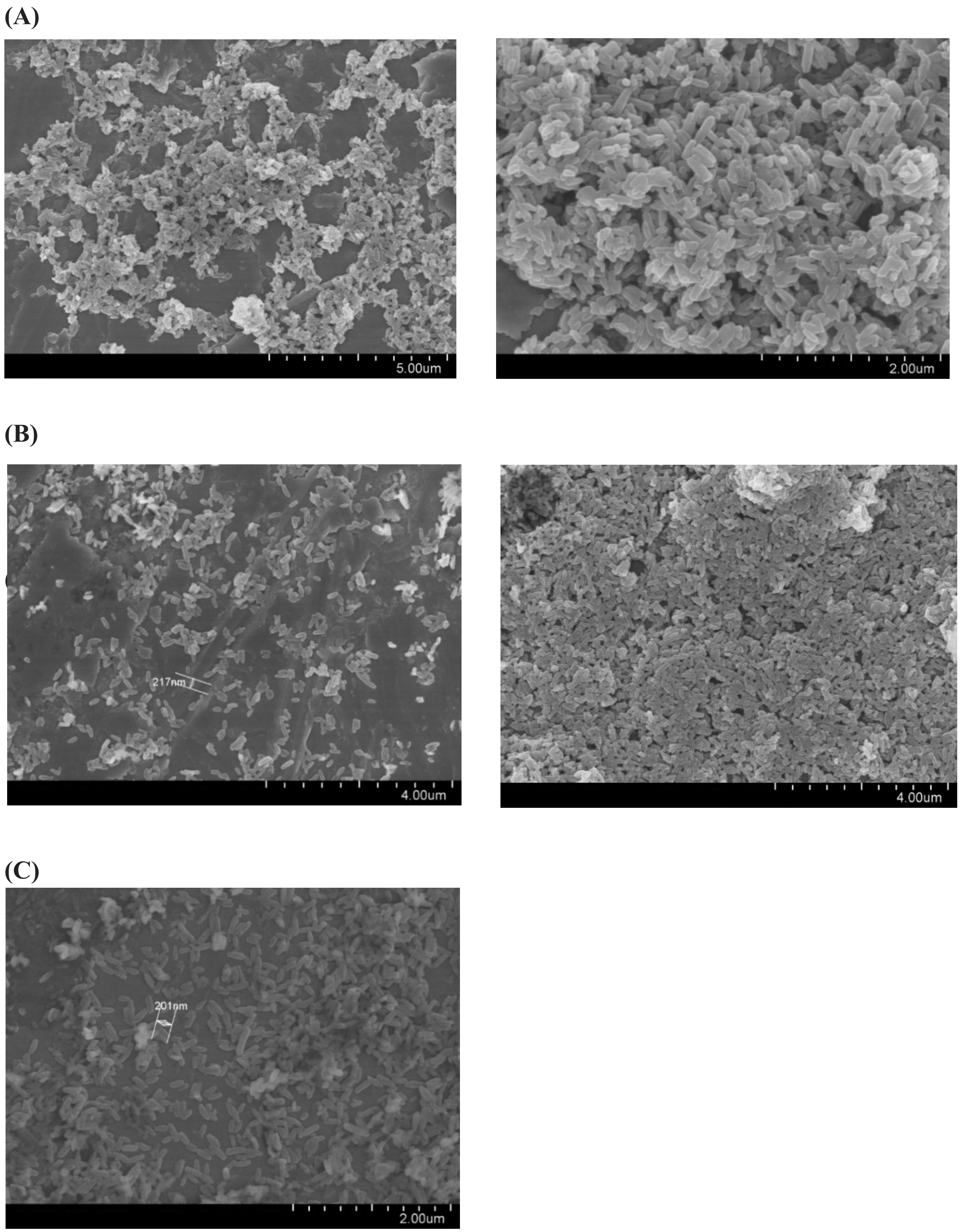

Figure S5. SEM images of three batches of Gd nano NU-1000. Sample A (top 2), Sample B (middle 2) and Sample C (bottom left). No change is observed in particle morphology after SALI.

MOF External Surface Area Calculations

Table S2. Comparison of Relative External Surface Area of MOFs and Gd(III) Complexes

Sample	MOF Surface Area (cm^2)	Gd(III) Complexes/Node	Area of Gd(III) Complexes[d] (cm^2)	Orders of Magnitude Difference
Gd NU-1000[a]	4.33×10^{-7}	0.93	24	8
Gd nano NU-1000[b]	7.95×10^{-10}	1.9	0.0038	7
Gd NU-901[c]	5.94×10^{-9}	1.4	0.034	7

[a]Modeled as a cylinder with 7 µM length and 0.375 µM in diameter

[b]Modeled as a cylinder 300 nm in length and 37.5 nm in diameter

[c]Modeled as a cylinder 550 nm in length and 137.5 nm in diameter

[d]Gd(III) complexes modeled as a sphere 1 nm in diameter

We approximated the shape of individual MOF particles as cylinders and that of the Gd(III) complex as a sphere. We calculated the external surface area of a single MOF particle for each sample using the parameters above and compared this value to the approximate area required to accommodate the amount Gd(III) complexes contained per MOF crystallite. We used volume of a MOF crystallite, the density of the MOF, and the Gd(III) complexes/node value determined by ICP-OES to number of Gd(III) complexes per MOF particle. We estimated that if spherical particles were arranged on a surface, they would require a circular area on that surface with a radius equivalent to that of the sphere. Thus, we were able to calculate the total surface area the complexes occupied on each MOF. We discovered that the total area in (cm^2) required to accommodate the Gd(III) complexes exceeded the external surface area of NU-1000 by 8 orders of magnitude. Similarly, the total surface area in (cm^2) required to accommodate the Gd(III) complexes exceeded the external surface of nano NU-1000 by 7 orders of magnitude. For the same calculation using NU-901, the Gd(III) complexes would require an area 7 orders of magnitude larger than the external surface area of NU-901.

These calculations comparing the external surface area of each MOF sample to the surface area required to accommodate the amount of Gd(III) complex supports other characterization evidence that points to significant amounts of Gd(III) occupying the pores of each MOF particle.

Diffuse Reflectance Infrared Spectra

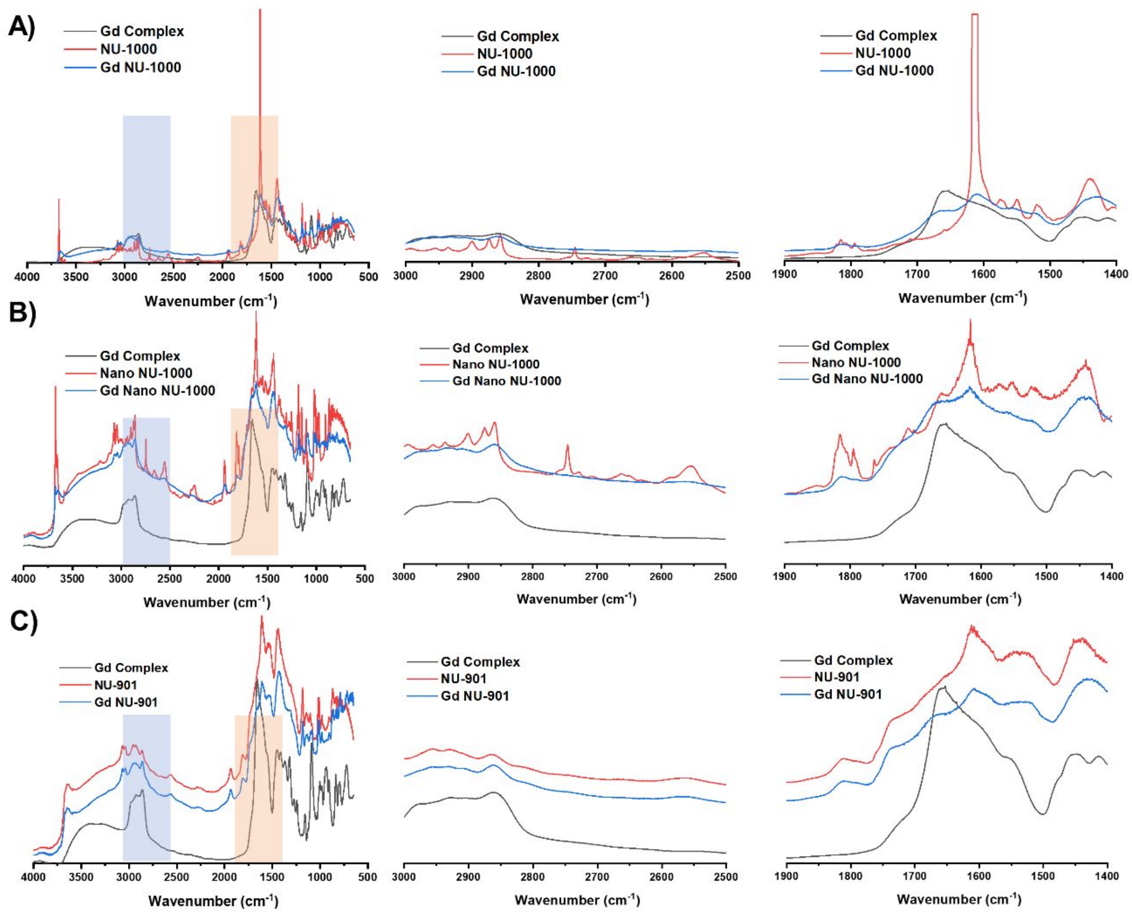

Figure S6. Experimental DRIFTS spectra of **A.** NU-1000 **B.** Nano NU-1000 and **C.** NU-901. Blue boxed region (2500-3000 cm^{-1}) is expanded in center frame and orange boxed region (1400-1900 cm^{-1}) is expanded on right frame.

STEM-EDS

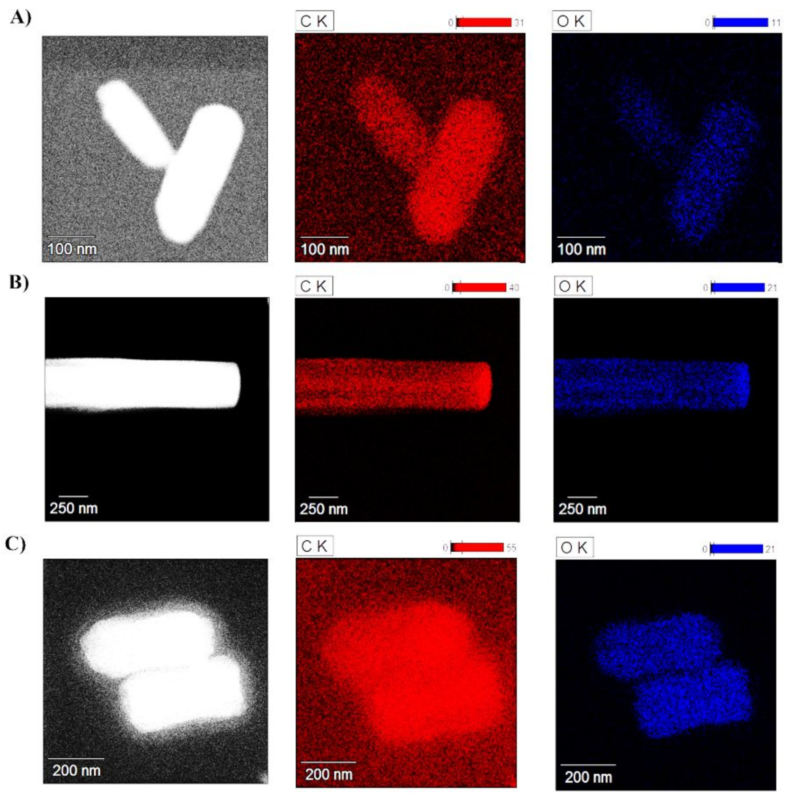

Figure S7. STEM-EDS data from each Gd(III)- MOF sample following SALI demonstrates uniform distribution of oxygen and carbon throughout the particle. **A.** Gd Nano NU-1000, **B.** Gd NU-1000, and **C.** Gd NU-901.

Stability Measurements in Water and Tris Buffer for 24 hrs

Stability of the hybrid materials in water and buffer was tested by suspending 5 mg Gd(III)-functionalized Zr-MOF conjugate in 10 mL of Millipore water and 10 mL tris buffer (150 mM NaCl, 50 mM Tris; pH 7.6). One sample of each Gd(III)-functionalized Zr-MOF was chosen and 5 mg of the hybrid material was used for each condition tested. Samples were incubated at 37 °C for 24 hr with constant agitation, then spun down and solvent exchanged with acetone 3x for 1 hr each. The final acetone supernatant was decanted, and the purified material was dried in a vacuum oven for 1 hour at 80 °C. Loading of Gd(III) complex was measured using ICP-OES. PXRD measurements were also taken to monitor crystallinity. The Gd(III) complex loading within each MOF sample decreased in both the water and tris buffered saline conditions. The Gd complex/node decreased by ~20% in both water and tris buffer for the Gd NU-1000 sample, ~16% in water and ~32% in tris buffer for the Gd nano NU-1000 sample, and ~25% in water and ~34% in tris buffer for the Gd NU-901 sample. The PXRD patterns indicate that bulk crystallinity was maintained after the exposure.

Table S3. Loading of Gd(III) complex in MOF series after soaking in water or tris buffer

Sample	Original Loading (Complexes/Node)	Water (Complexes/Node)	Tris (Complexes/Node)
Gd NU-1000	0.97	0.76	0.78
Gd nano NU-1000	2.05	1.72	1.40
Gd NU-901	1.45	1.09	0.96

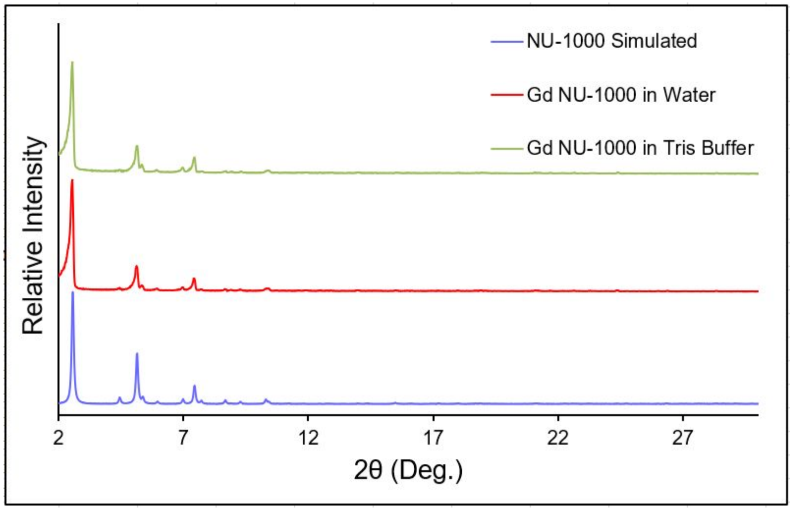

Figure S8. PXRD patterns for Gd (III) NU-1000 series after soaking in water or tris buffer for 24 hr at 37°C.

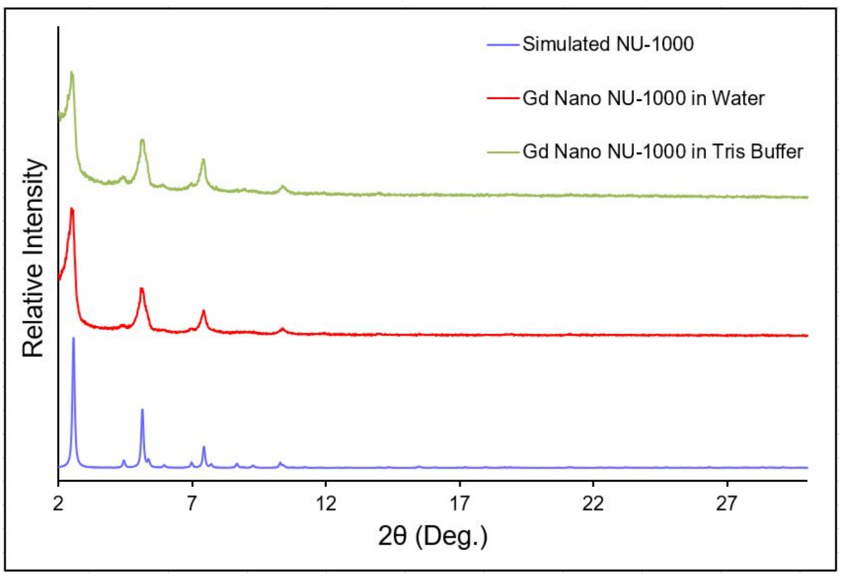

Figure S9. PXRD patterns for Gd (III) nano NU-1000 series after soaking in water or tris buffer for 24 hr at 37°C.

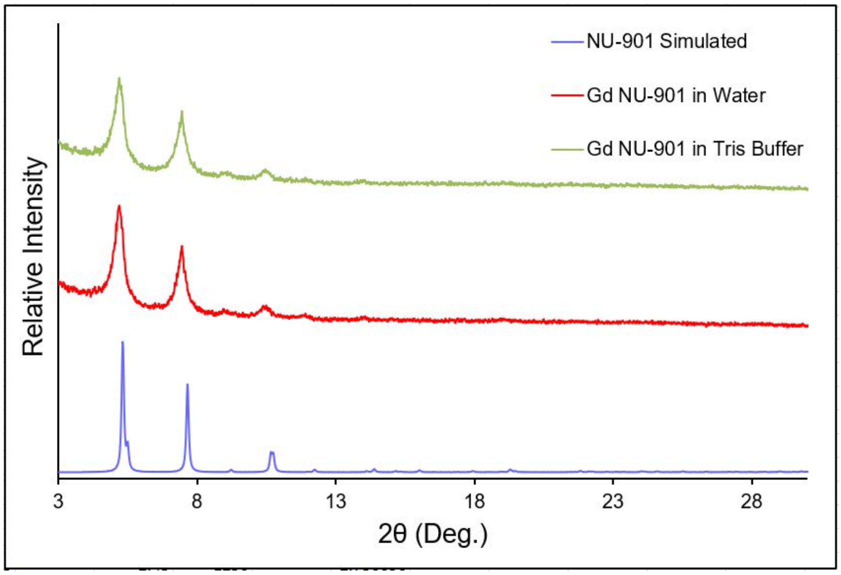

Figure S10. PXRD patterns for Gd (III) NU-901 series after soaking in water or tris buffer for 24 hr at 37°C.

Stability Measurements in Water for 24 hr-72 hr

Stability of the hybrid materials in water was tested from 24 hr-72 hr by suspending 5 mg of each Gd(III)-functionalized Zr-MOF sample in 10 mL of Millipore water. One sample of each Gd(III) MOF was chosen and 5 mg of the hybrid material was tested at 24 hr, 48 hr, and 72 hr for a total of nine measurements. Samples were incubated at 37 °C for 24 hr, 48 hr, and 72 hr with constant agitation, spun down and solvent exchanged with acetone 3x for 1 hr each. The final acetone supernatant was decanted, and the purified material was dried in a vacuum oven for 1 hour at 80 °C. Loading of Gd(III) complex was measured using ICP-OES. PXRD measurements were taken of the 48 hr time points to monitor crystallinity. While the Gd(III) loading within each sample decreased at the 24 hr time point, it did not change significantly at the 48 hr or 72 hr time points. The Gd complex/node decreased by ~25% in 24 hr, 32% in 48 hr, and 31% in 72 hr for the Gd NU-1000 sample, indicating that the uncoordinated Gd(III) removed from the sample occurs within the first 24 hr. For the nano Gd NU-1000 sample the Gd complex/node decreased by ~14% in 24 hr and remained steady for both the 48 hr and 72 hr time points. The same is true for the Gd NU-901 sample. In the first 24 hr, the Gd complex/node decreased by ~29% and then remained steady for both the 48 hr and 72 hr time points.

Table S4. Loading of Gd(III) complex in MOF series after soaking in water for 24, 48, or 72 hr

Sample	Original Loading (Complexes/Node)	24 hr Loading (Complexes/Node)	48 hr Loading (Complexes/Node)	72 hr Loading (Complexes/Node)
Gd NU-1000	0.97	0.73	0.66	0.67
Gd nano NU-1000	2.05	1.76	1.76	1.72
Gd NU-901	1.45	1.03	1.05	1.00

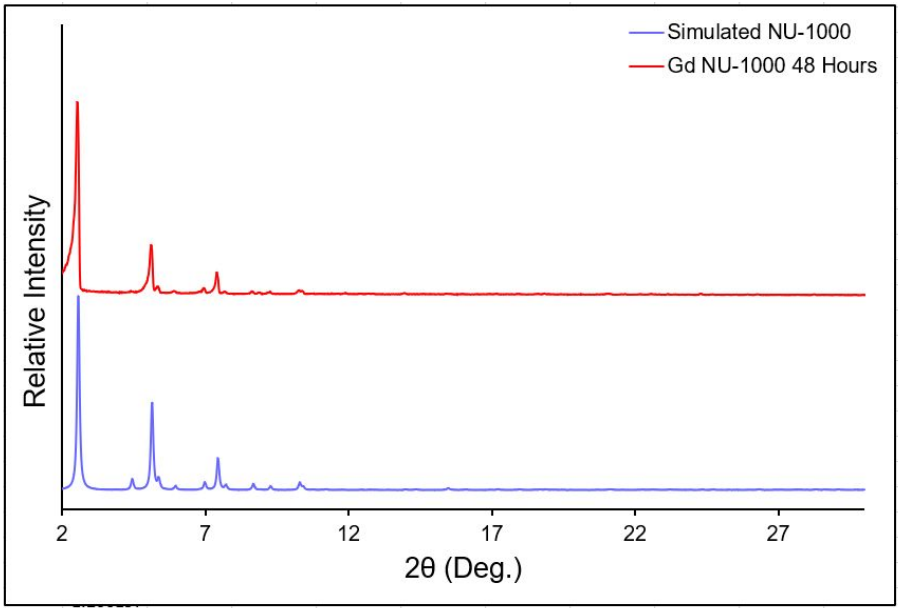

Figure S11. PXRD pattern for Gd (III) NU-1000 after soaking in water for 48 hr at 37°C.

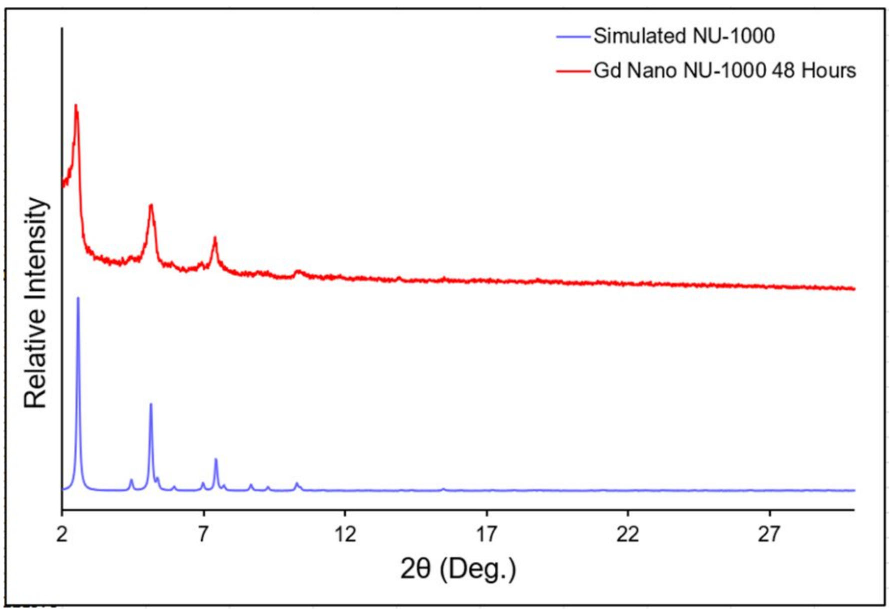

Figure S12. PXRD pattern for Gd (III) nano NU-1000 after soaking in water for 48 hr at 37°C.

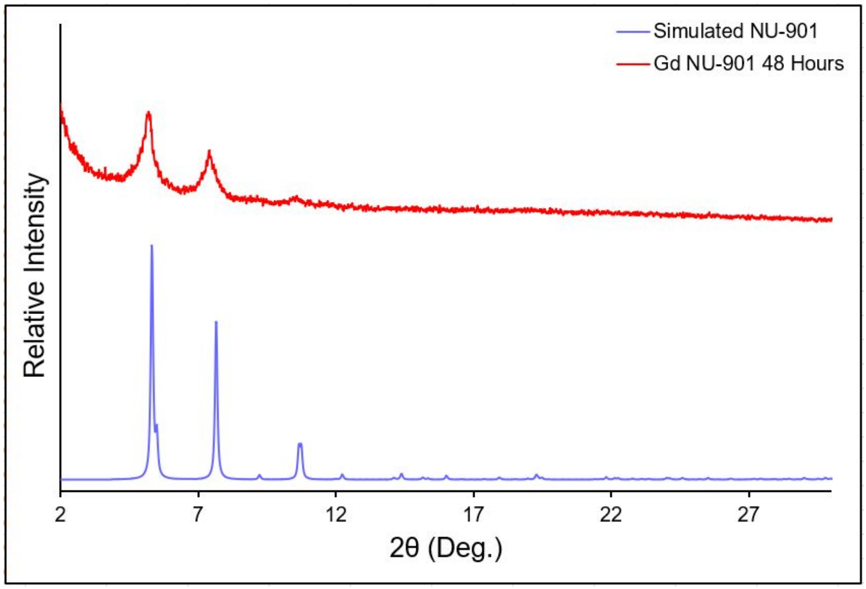

Figure S13. PXRD pattern for Gd (III) NU-901 after soaking in water for 48 hr at 37°C.

Stability Measurements in Water: Volume Dependence

Stability of hybrid material was tested by suspending 5 mg of each Gd(III)-functionalized Zr-MOF sample in 10, 20, or 40 mL of Millipore water to investigate whether there was volume dependent leaching of the Gd complex from the hybrid materials. One sample of each Gd(III)-functionalized Zr-MOF was tested at 10 mL, 20 mL, and 40 mL for a total of nine measurements. Samples were incubated at 37 °C for 24 hr with constant agitation and spun down and solvent exchanged with acetone 3x for 1 hr each. Following the final acetone solvent exchange, the purified material was dried in a vacuum oven for 1 hr at 80 °C. Loading of Gd(III) complex was measured using ICP-OES. The data indicates there is no relationship between the volume of water used to wash the sample and the amount of Gd(III) leached from the material. While some percentage of Gd(III) was removed from each sample tested, the amount did not significantly change as the volume of water increased. The number of Gd complexes per node of MOF in the Gd NU-1000 sample decreased by ~25% in 10 mL, 27% in 20 mL, and 25% in 40 mL, which indicates that there is no volume dependence on the amount of Gd washed from the sample. For the nano Gd NU-1000 sample, the Gd complex per node of MOF decreased by ~17% when exposed to 10 mL of water, ~24% when exposed to 20 mL of water, and ~28% when exposed to 40 mL of water. The same slight decreasing trend holds true for the Gd NU-901 sample. The Gd(III) loading decreased by

~30% when exposed to 10 mL of water, ~33% when exposed to 20 mL of water, and ~37% when exposed to 40 mL of water.

Table S5. Loading of Gd(III) complex in MOF series after soaking in 10, 20, or 40 mL water

Sample	Original Gd(III) Loading (Complexes/Node)	10 mL Loading (Complexes/Node)	20 mL Loading (Complexes/Node)	40 mL Loading (Complexes/Node)
Gd NU-1000	0.97	0.73	0.71	0.73
Gd nano NU-1000	2.05	1.70	1.56	1.47
Gd NU-901	1.45	1.02	0.97	0.92

Modified Solvent Exchange Procedure Following SALI

Based on the results from the previous three tests, we hypothesized that the extra solvent exchanges in water after the initial SALI procedure to incorporate Gd(III) into the MOF particles was removing excess uncoordinated Gd(III) complexes from the hybrid materials. To test this hypothesis, we resynthesized the Gd(III)-functionalized Zr-MOF materials and increasing the number of solvent exchanges following the SALI process of the Gd(III) complex into each MOF until there was ≤ 6 ppm of Gd(III) in the supernatant. This concentration of Gd(III) was determined by ICP-OES. Therefore, the procedure follows the original SALI method described in the experimental section of the main text with only one change, when the reaction mixture was removed from the oven it was solvent exchanged with 10 mL of Millipore water 3x for 10 min. each. Then, the material was resuspended in water and shaken at 37 °C for 2 hr. The Gd(III) concentration in the supernatant was measured using ICP-OES after this solvent exchange (procedure described below) and repeated until ≤ 6 ppm of Gd(III) remained in the supernatant. This typically required 5 total washes. Following the final solvent exchange, the supernatant was exchanged for 10 mL of acetone and the Gd MOF material was soaked for 18 hr in acetone before drying in a vacuum oven at 80°C and characterized using PXRD, N_2 isotherm, and SEM.

ICP-OES Sample Preparation for Supernatant

Metal analysis by ICP-OES followed the procedure described in the main text. Additionally, the supernatant from the new solvent exchange procedure was filtered through a 0.20 µm syringe to remove any residual MOF that remained suspended before ICP-OES. Any free Gd(III) complexes in the solvent are small enough to pass through the filter. Then, 300 µL of this filtered supernatant was digested in 300 µL concentrated trace nitric acid (> 69%, Thermo Fisher Scientific, Waltham, MA, USA) and placed at 65 °C for at least 3 hours to allow for complete sample digestion. Ultra-pure H_2O (18.2 MΩ·cm) was then added to produce a final solution of 3.0% nitric acid in a total sample volume of 10 mL. The rest of the data acquisition and work-up followed the original method.

Characterization of Gd MOF Materials After New Solvent Exchange Procedure

The characterization for the Gd MOF materials after this new solvent exchange procedure include ICP-OES, ICP-MS, sorption, PXRD, and relaxivity at 1.4 T.

Table S6. Loading of Gd(III) complex in MOF series with modified solvent exchange procedure

Sample	Loading – Original Solvent Exchange Method (Complexes/Node)	Loading – New Solvent Exchange Method (Complexes/Node)	Final Wash [Gd] (ppm)	% of Gd Exposure Removed
Gd NU-1000	0.93 +/- 0.04	1.2	4.3	27.9
Gd nano NU-1000	1.9 +/- 0.1	2.0	6.3	18.5
Gd NU-901	1.4 +/- 0.1	0.63	3.3	37.9

The Gd(III) complex loading for the NU-1000 and nano NU-1000 samples did not vary significantly between the two solvent exchange methods, but was significantly lower for NU-901 with the new method.

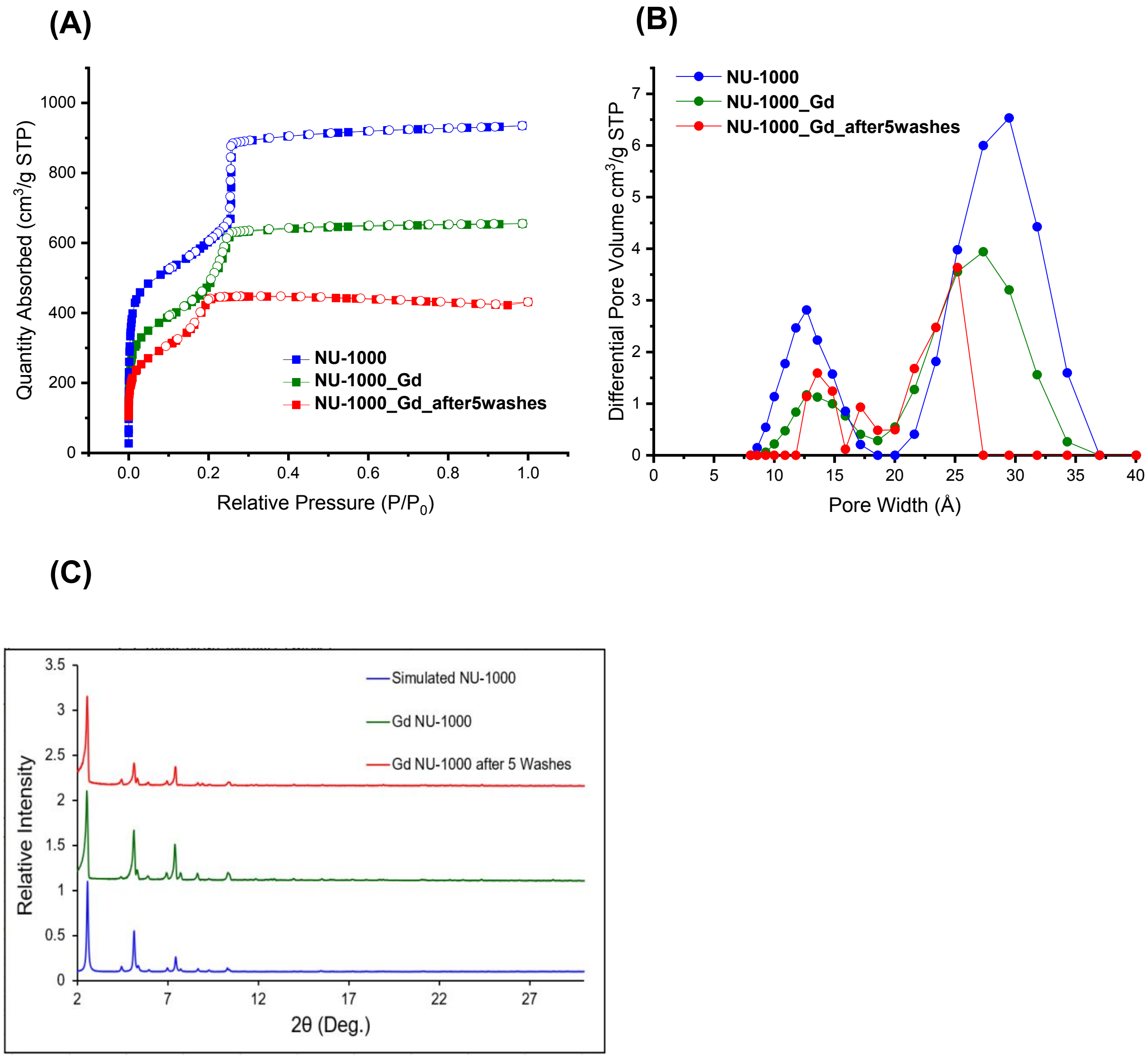

Figure S14. Characterization of Gd NU-1000 synthesized with the new solvent exchange procedure. (A) N_2 isotherms and (B) corresponding pore size distributions show decreased BET surface area and pore width with the new synthesis compared to the original method of solvent exchange (BET Surface Area of NU-1000 after washing = 1,160 m²/g). (C) PXRD pattern of Gd NU-1000 shows agreement with simulated and unfunctionalized MOF, indicating that bulk crystallinity of the MOF is maintained.

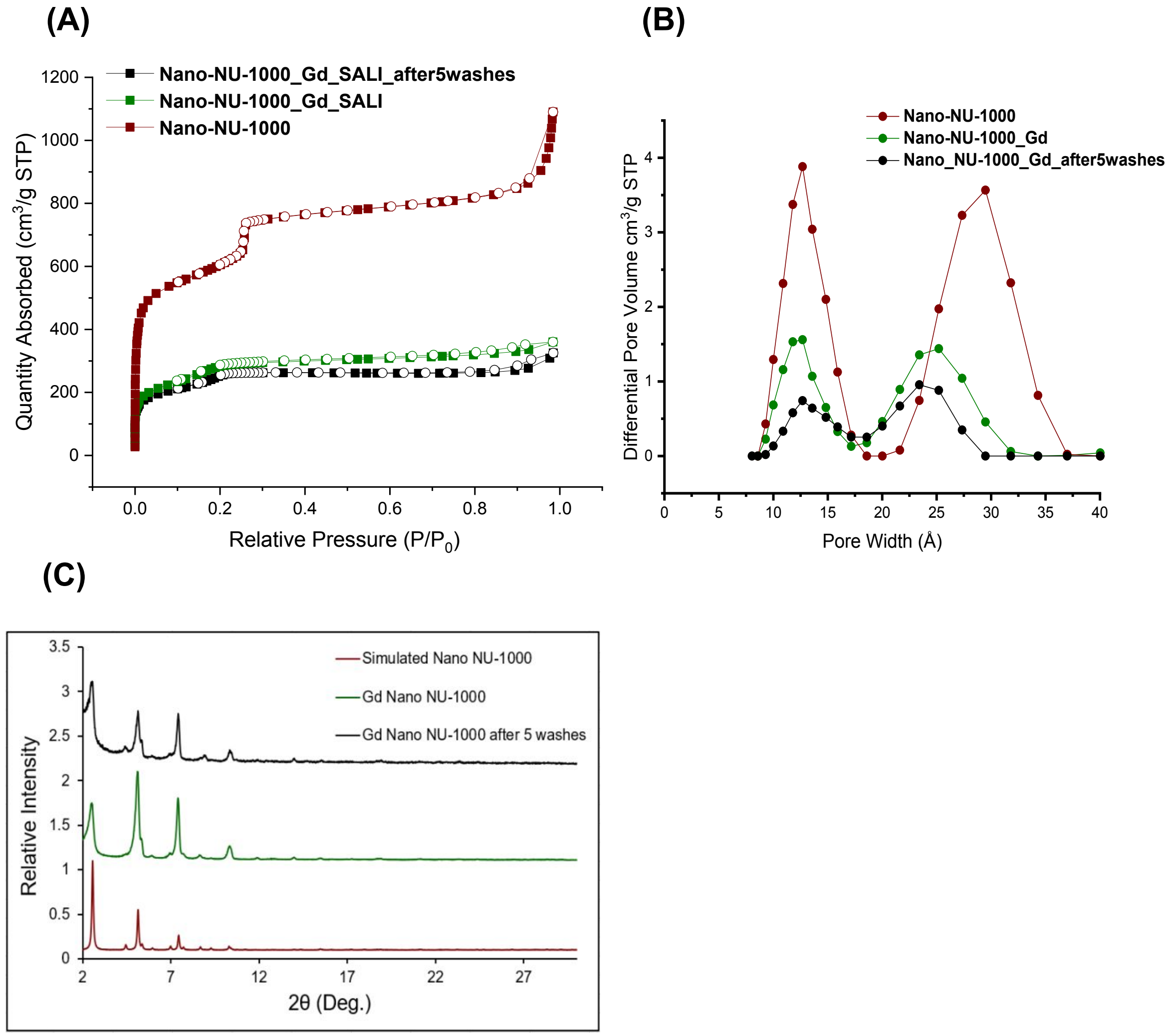

Figure S15. Characterization of Gd nano NU-1000 synthesized with the new solvent exchange procedure. (A) N_2 isotherms show similar agreement with the new solvent exchange process compared to the original method of solvent exchange (BET Surface Area of Nano NU-1000 after washing = 820 m^2/g). (B) The corresponding pore size distributions show a slight decrease in pore volume, but the pore widths remain unchanged. (C) The PXRD pattern of Gd nano NU-1000 demonstrates agreement with the simulated and unfunctionalized MOF patterns, indicating that the bulk crystallinity of the structure is maintained.

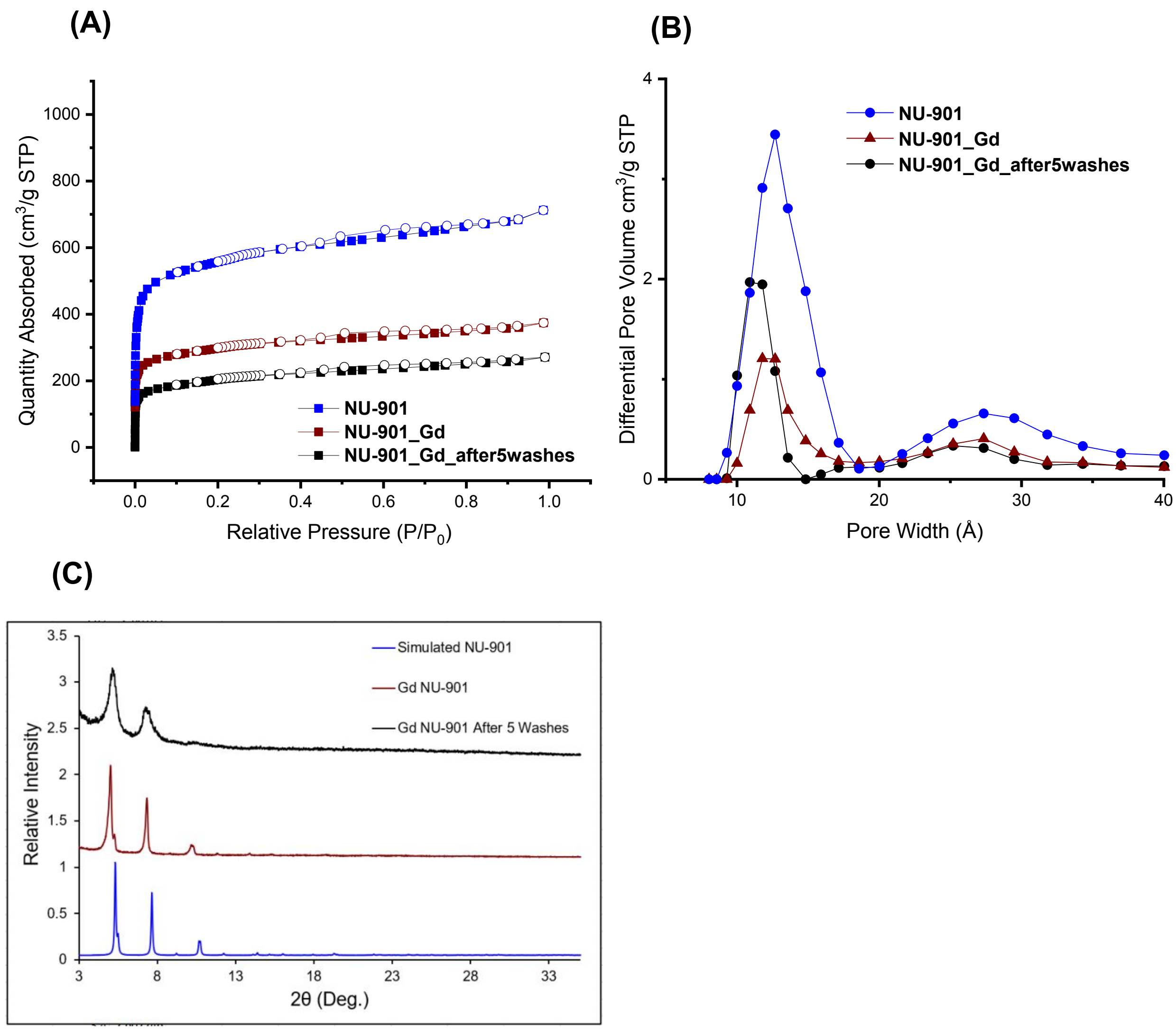

Figure S16. Characterization of Gd NU-901 synthesized with the new solvent exchange procedure. (A) N_2 isotherms and (B) corresponding pore size distributions show a decreased BET surface area and pore volume with the modified solvent exchange process as compared to the original method of solvent exchange (BET Surface Area of NU-901 after 5 washes = 740 m²/g). (C) PXRD pattern of Gd NU-901 shows agreement with simulated and unfunctionalized MOF, although there is some peak broadening occurring in the sample, indicating that while the bulk crystallinity of the MOF is maintained, the number of defects introduced during this process may be increasing.

Table S7. Per Gd(III) relaxivity at 1.4 T for Gd(III)-functionalized Zr-MOF series with new solvent exchange method

Sample	r_1 **(mM^{-1}s^{-1})**	r_2 **(mM^{-1}s^{-1})**
Gd-C5-COOH	6.4	10.4
Avg. for Gd NU-1000 (original)	6.4 +/- 0.8	12 +/- 1
Gd NU-1000 Washed	4.6	10
Avg. for Gd nano NU-1000 (original)	26 +/- 1	53 +/- 2
Gd Nano NU-1000 Washed	29	56
Avg. for Gd NU-901 (original)	16 +/- 1	30 +/- 3
Gd NU-901 Washed	18	36

Despite some differences in Gd(III) complex loading for NU-901, both methods of solvent exchange result in similar per Gd(III) relaxivity values in each of the three MOFs. We hypothesize that while the modified solvent exchange process may remove unbound excess Gd(III) complexes from the samples, these complexes must not contribute significantly to the observed relaxivity in these hybrid materials. Thus, while the per particle relaxivity is reduced with lower loading, the ionic (i.e. per Gd(III)) relaxivity is unchanged.

Relaxivity Controls at 1.4 T

Stock suspensions of unfunctionalized nano NU-1000 and NU-901 MOF sample were made by suspending ~1 mg of material in 1 mL of Millipore water. This sample was serially diluted four times, generating five samples of 500 µL, which were then heated to 37 °C. Relaxation times were measured on a Bruker mq60 NMR analyzer equipped with Minispec v 2.51 Rev.00/NT software (Bruker Biospin, Billerica, MA, USA) operating at 1.41 T (60MHz) and 37 °C. Measurement of T_1 relaxation times were made using an inversion recovery pulse sequence with the following parameters: 4 scans per point, 10 data points, mono-exponential curve fitting, phase cycling, 10 ms first pulse separation, and a recycle delay and final pulse separation $\geq 5\ T_1$. Measurement of T_2 relaxation times were made using the Carr-Purcell-Meiboom-Gill (CPMG) pulse sequence. The inverse of the relaxation time ($1/T_1$ or $1/T_2$, s^{-1}) was plotted against the Zr concentration (mM) determined by ICP-OES for each of the five samples. Per node relaxivity of unfunctionalized MOF was calculated using the concentration of Zr_6 and per node relaxivity of MOF loaded with Gd-C5-COOH complex calculated by multiplying ionic relaxivity by loading per node. By applying a linear fit to this data, the slope generated was defined as the relaxivity (r_1, r_2) of the agent in units of $mM^{-1}\ s^{-1}$. The unfunctionalized MOF has no contribution to r_1 and insignificant contributions to r_2. Further relaxivity controls were not pursued based on these results.

Table S8. Relaxivity Control Measurements at 1.4 T

Sample	r_1 ($mM^{-1}s^{-1}$)	r_2 ($mM^{-1}s^{-1}$)
Gd-C5-COOH	6.4	10.4
Average for Gd nano NU-1000	26 +/- 1	53 +/- 2
nano NU-1000 MOF (per node)	0.0	2.2
Gd nano NU-1000 (per node)	49	101
Average for Gd NU-901	16 +/- 1	30 +/- 3
NU-901 MOF (per node)	0.0	2.1
Gd NU-901 (per node)	22	42

NMRD Best Fit Parameters

Values for the electronic parameters Δ_t, τ_v and ZFS are very close between Gd(III) nano NU-1000 and Gd(III) NU-901. The main difference in fit comes from τ_m and outer sphere relaxation contributions.

Table S9. Best fit parameters at 25°C

25 °C	nanoNU1000	NU901
τ_R (ns)	>10	>10
Δ_t (cm^{-1})	0.02	0.02
τ_v (ps)	18	21
τ_M (μs)	0.90	3.0
ZFS (cm^{-1})	0.052	0.057
d (Å)	3.6	-

r = 3.05 Å, q = 2, D = 2.4 × 10^{-9} m^2/s, $\theta_{ZFS} = 68°$

Table S10. Best fit parameters at 37°C

37 °C	nanoNU1000	NU901
τ_R (ns)	>10	>10
Δ_t (cm^{-1})	0.02	0.018
τ_v (ps)	14	20
τ_M (μs)	0.85	2.6
ZFS (cm^{-1})	0.052	0.057
d (Å)	3.6	-

r = 3.05 Å, q = 2, D = 3.3 × 10^{-9} m^2/s, $\theta_{ZFS} = 68°$

Preliminary Characterization of Gd MOF-808

Synthesis and characterization of MOF-808 followed literature procedure.[8] Functionalization of MOF-808 with Gd-C5-COOH followed the same SALI procedure described in the main text. Loading by ICP-OES was found to be *0.83 complexes/node*. The material was characterized by PXRD and sorption analysis.

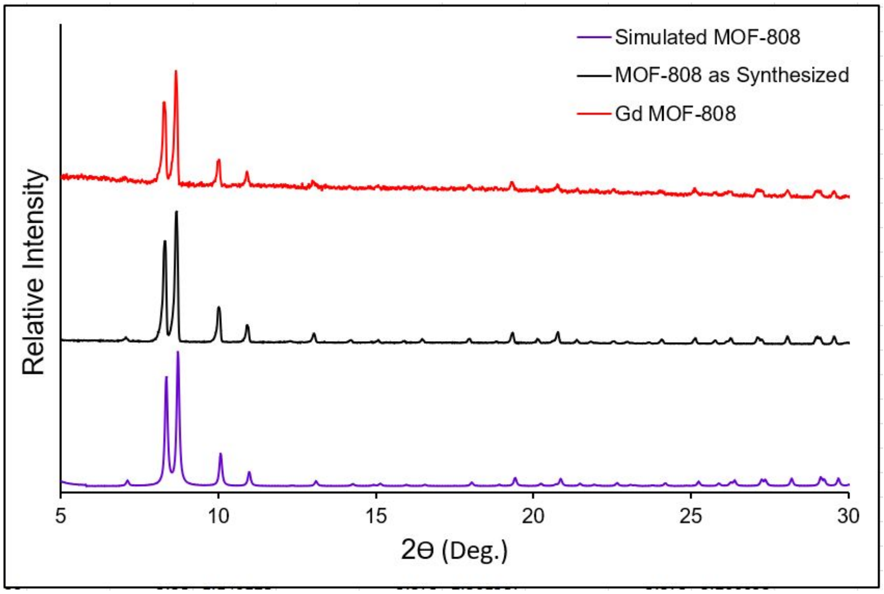

Figure S17. PXRD patterns of MOF-808 post-SALI. Patterns show that crystallinity is maintained after functionalization with the Gd(III) complex.

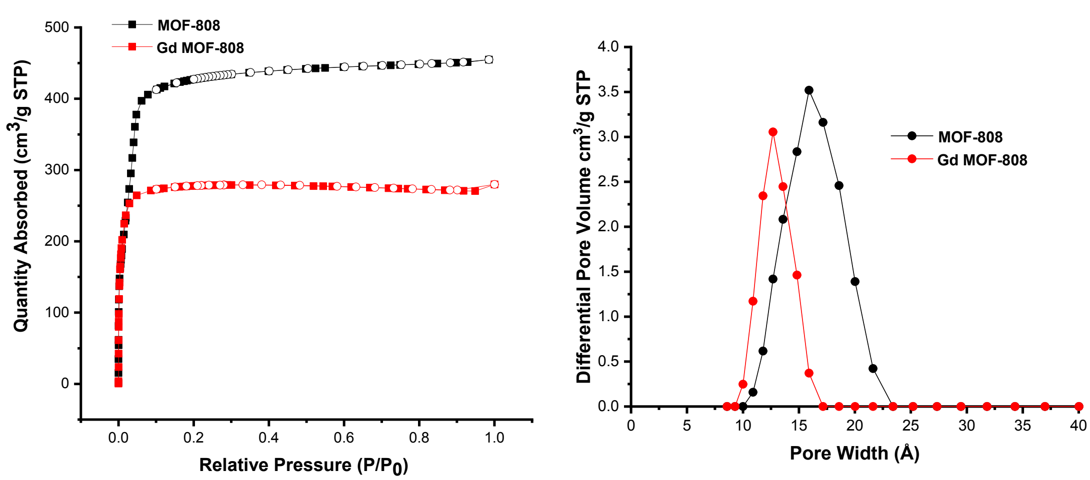

Figure S18. Gd NU-1000 N_2 isotherms and corresponding pore size distributions show decreased BET surface area and pore width following Gd(III) incorporation using SALI.

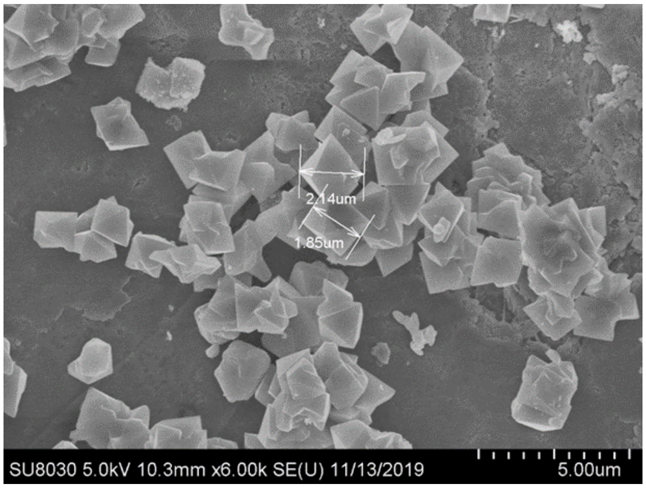

Figure S19. SEM image of unfunctionalized MOF-808 with particle size ~1.8-2.5 μm.

Relaxivity at 1.4 T was measured for Gd MOF-808, yielding values of $r_1 = 5.1$ mM^{-1}s^{-1} and $r_2 = 9.3$ mM^{-1}s^{-1}, the worst among the MOF series. NMRD analysis also highlighted the especially poor performance of Gd MOF-808.

The ^{1}H NMRD profile of Gd-MOF-808 was collected at 25 °C. For this complex, the profile does not show any high field peak, thus indicating fast rotation conditions. The relaxivity is very low for a q=2 Gd(III) complex, pointing to slow exchange conditions. The profile was fit according to the Solomon-Bloembergen-Morgan (SBM) model, assuming two water molecules regularly coordinated to the Gd ion, and including outer-sphere contributions to relaxation. When the latter is modeled assuming a distance of closest approach, d, of 3.6 Å and a diffusion coefficient, D, of 2.4×10^{-9} m^2/s, the calculated profile decreases more slowly with increasing the magnetic field than indicated by the experimental data (dotted line in **Fig. S20**). Therefore, in order to better reproduce the experimental profile, the outer-sphere contribution to the relaxivity was decreased, assuming that the solid angle in which the water molecules can approach the Gd(III) ion till the distance of closest approach is restricted to about 38% of the whole sphere (solid line in **Fig. S20**). The corresponding best fit parameters are reported in **Table S11**.

This challenge in modeling the outer-sphere contributions to relaxivity supports our hypothesis that the small, cage-like pores of MOF-808 further inhibits water exchange and hydration of the Gd(III) ion compared to channel-type MOFs.

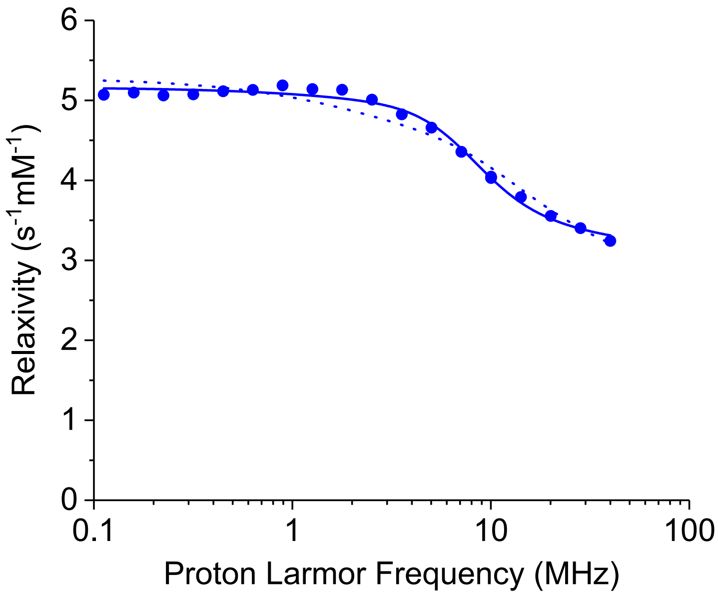

Figure S20. Experimental ^{1}H NMRD profile of Gd-MOF-808 at 25 °C and best fit profiles calculated with the parameters reported in Table S11.

Table S11. Best fit parameters obtained from the fit of the experimental ^{1}H NMRD profile of Gd-MOF-808 at 25 °C

	MOF808	
	A. Dotted line	B. Solid line
τ_R (ps)	37	51
Δ_t (cm^{-1})	0.037	0.040
τ_v (ps)	20 (fixed)	20 (fixed)
τ_M (μs)	23	4.5
Fraction outer-sphere	100% (fixed)	38%
d (Å)	3.6 (fixed)	3.6 (fixed)
q	2 (fixed)	2 (fixed)
r (Å)	3.05 (fixed)	3.05 (fixed)
D [m^2/s]	2.4×10^{-9} (fixed)	2.4×10^{-9} (fixed)

Assuming that water diffuses to a distance of minimum approach all around the complex (dotted line), or only within a solid angle which is much smaller than spherical (solid line). The corresponding profiles are shown in **Fig. S20** as dotted and solid lines.

References

1. Islamoglu, T.; Otake, K.-i.; Li, P.; Buru, C. T.; Peters, A. W.; Akpinar, I.; Garibay, S. J.; Farha, O. K., Revisiting the Structural Homogeneity of NU-1000, a Zr-Based Metal–Organic Framework. *CrystEngComm* **2018,** *20* (39), 5913-5918.

2. Li, P.; Klet, R. C.; Moon, S.-Y.; Wang, T. C.; Deria, P.; Peters, A. W.; Klahr, B. M.; Park, H.-J.; Al-Juaid, S. S.; Hupp, J. T.; Farha, O. K., Synthesis of Nanocrystals of Zr-Based Metal–Organic Frameworks With csq-net: Significant Enhancement in the Degradation of a Nerve Agent Simulant. *Chem. Commun. (Cambridge, U.K)* **2015,** *51* (54), 10925-10928.

3. Garibay, S. J.; Iordanov, I.; Islamoglu, T.; DeCoste, J. B.; Farha, O. K., Synthesis and Functionalization of Phase-Pure NU-901 for Enhanced CO2 Adsorption: The Influence of a Zirconium Salt and Modulator on the Topology and Phase Purity. *CrystEngComm* **2018,** *20* (44), 7066-7070.

4. Rowe, M. D.; Chang, C.-C.; Thamm, D. H.; Kraft, S. L.; Harmon, J. F.; Vogt, A. P.; Sumerlin, B. S.; Boyes, S. G., Tuning the Magnetic Resonance Imaging Properties of Positive Contrast Agent Nanoparticles by Surface Modification with RAFT Polymers. *Langmuir* **2009,** *25* (16), 9487-9499.

5. Hatakeyama, W.; Sanchez, T. J.; Rowe, M. D.; Serkova, N. J.; Liberatore, M. W.; Boyes, S. G., Synthesis of Gadolinium Nanoscale Metal−Organic Framework with Hydrotropes: Manipulation of Particle Size and Magnetic Resonance Imaging Capability. *ACS Appl. Mater. Interfaces* **2011,** *3* (5), 1502-1510.

6. Carné-Sánchez, A.; Bonnet, C. S.; Imaz, I.; Lorenzo, J.; Tóth, É.; Maspoch, D., Relaxometry Studies of a Highly Stable Nanoscale Metal–Organic Framework Made of Cu(II), Gd(III), and the Macrocyclic DOTP. *J. Am. Chem. Soc.* **2013,** *135* (47), 17711-17714.

7. Peller, M.; Böll, K.; Zimpel, A.; Wuttke, S., Metal–Organic Framework Nanoparticles for Magnetic Resonance Imaging. *Inorg. Chem. Front.* **2018,** *5* (8), 1760-1779.

8. Drout, R. J.; Howarth, A. J.; Otake, K.-i.; Islamoglu, T.; Farha, O. K., Efficient Extraction of Inorganic Selenium from Water by a Zr Metal–Organic Framework: Investigation of Volumetric Uptake Capacity and Binding Motifs. *CrystEngComm* **2018,** *20* (40), 6140-6145.